Laboratoire de Physique Corpusculaire
de Clermont-Ferrand

A Study of QMM Hysteresis Cycle Data: Field Linearity and Field Reproducibility

QMM Collaboration, August 1997
Quadrupole Magnetic Measurements

P. Vernin

DAPNIA/SPhN
CEA-Saclay
91191 GIF-SUR-YVETTE CEDEX France

H. Fonvieille, G. Quéméner

Laboratoire de Physique Corpusculaire
de Clermont-Ferrand
IN2P3/CNRS - Université Blaise Pascal
63177 AUBIERE CEDEX France

PCCF RI 9713

A study of QMM Hysteresis Cycle Data: Field Linearity and Field Reproducibility

QMM Collaboration, August 1997

Quadrupole Magnetic Measurements

P. Vernin
CEA-Saclay
H. Fonvieille, G. Quéméner
LPC-Clermont-Fd

This note contains a study of the hysteresis data provided by the quadrupole field mapping of the HRS Electron Arm.

The data was taken in june-july 1996 by the QMM Collaboration. For each quad Q1, Q2, Q3, a series of runs was performed to obtain the hysteresis curve of the magnet at maximal current. These runs are indeed the major part of our data set, i.e. the part that yields the final 3D field maps of the quads.

The focus of the present document is not the field maps but a specific analysis of QMM data in terms of hysteresis curves, and field linearity as a function of the current. Also, our measurements allow to put limits on the reproducibility of magnet setting for the presently used operating mode of the quads. The main results are summarized in fig. 8 and section 5.

1 Field Integrals: $\mathbf{F}_{meas}(i)$ and $\mathbf{F}_{model}(i)$

We will work with *field integrals*, i.e. $\int B.dl$ in units of Tesla.millimeters. A general notation for a field integral will be F.

A main feature of the QMM mapping device is its axially segmented probe, divided into ten rotating coils. This segmentation is fully used for making 3D field maps. Here we shall only use data obtained by summing the information of the ten coils, i.e. integrating over the whole length of the magnet, including the fringe field regions. This measured flux can be expressed directly in terms of a field integral. The actual definition of F is the following:

$\mathbf{F}_{meas}(I)$ = *field integral measured by QMM, over the ten coils* [1], *at magnet current I, for the Normal Quadrupole Harmonic, in T.mm, at radius* $r_{ref} = 150$ *mm for Q1 and 300 mm for Q2/Q3.*

We also use a reference model of the magnets. It is based on the geometry of the superconducting wires, and provides a model field integral F_{model} for comparison with the measurement.

$F_{model}(I_{ref})$ = *field integral given by the model, over the ten coils, at a reference current* I_{ref} *in the magnet, for the Normal Quadrupole Harmonic, in T.mm, at radius* r_{ref}. $I_{ref} = 3250$ *A for Q1 and 1850 A for Q2/Q3.*

Whereas the real magnets have non-zero hysteresis and may exhibit non-linearity effects with the current, the model has zero hysteresis and is fully linear:

[1] All numerical values in this document are for chamfered coils. Therefore numbers may differ from the ones quoted in "Preliminary Results of Magnetic Measurements of Electron Arm HRS Quadrupoles", QMM Note, July 15th 1996.

Q1	F_{meas} at I= 3250 A is +1178 T.mm F_{model} at I= 3250 A is +1162 T.mm
Q2	F_{meas} at I= 1850 A is -1813 T.mm F_{model} at I= 1850 A is -1799 T.mm
Q3	F_{meas} at I= 1600 A is -1566 T.mm F_{model} at I= 1600 A is -1556 T.mm

Table 1: Typical field integrals for the 2N-harmonic (Normal Quadrupole).

$F_{model}(I = 0) = 0.$
$F_{model}(I) = F_{model}(I_{ref}) \times I/I_{ref}$.

Typical measured and model field integrals for Q1, Q2, Q3 are indicated in Table 1. More accurate numbers can be found in Appendix I. In particular Table 4 contains the actual measured values from which all the plots and numbers in this document have been produced. The Appendix also contains a discussion of the error bar on the QMM measurements.

2 Cycling sequences of QMM data taking

Prior to a measurement step by step on the hysteresis loop, each magnet was put in a "clean state" by cycling it once (going to $+I_{max}$ and $-I_{max}$). Then, QMM data taking could start when back to the setpoint at $\pm I_{max}$.

Table 2 shows the sequence that was done for each quad. One notices that for Q3, the cleaning cycle was mistakenly closed at +1200 A instead of +1600 A. Measurements were thus performed on an asymmetric cycle (I = +1200/0/-1600/0/+1200 A) even if a supplementary last point is quoted at +1600 A. Also, the maximal current for Q3 was limited to ± 1600 A, due to quench problems at higher current.

Q1 cleaning sequence	0 → +2000 → +3250 → 0 → -2000 → -3250 Amperes
Q1 measuring sequence	-3250 → -3000 → -2000 → -1000 → 0 → +1000 → → +2000 → +3000 → +3250 → +3000 → +2000 → → +1000 → 0 → -1000 → -2000 → -3000 → -3250 Amperes
Q2 cleaning sequence	0 → +1850 → +1200 → 0 → -1200 → -1850 → → -1200 → 0 → +1200 → +1850 Amperes
Q2 measuring sequence	+1850 → +1600 → +1200 → +800 → +400 → 0 → → -400 → -800 → -1200 → -1600 → -1850 → -1600 → → -1200 → -800 → -400 → 0 → +400 → +800 → → +1200 → +1600 → +1850 Amperes
Q3 cleaning sequence	0 → +1600 → 0 → -1600 → 0 → +1200 Amperes
Q3 measuring sequence	+1200 → +1000 → +800 → +600 → +400 → 0 → → -200 → -400 → -800 → -1200 → -1600 → -1200 → → -800 → -400 → 0 → +400 → +800 → +1200 → → +1600 Amperes

Table 2: Cleaning and Cycling sequences during QMM data taking (june-july 1996)

3 Hysteresis Curves: choice of representation

A hysteresis loop has the general form displayed in **fig. 1**. At I=0 one can see the non-zero field of the magnet. For the HRS quads it is the sum of a remanent field (due to the iron yoke) and a persistent field (due to the superconducting coils). **Fig. 3** shows the curves obtained for the HRS quads for $\int B.dl$ versus I : obviously this is not a suitable representation for a detailed hysteresis study, as the area within the loop is not visible.

Instead, one must work with a differential variable such as:

$$y(I) \;=\; \int B_{meas}(I).dl \;-\; \int B_{model}(I).dl \;=\; F_{meas}(I) \;-\; F_{model}(I)$$

where the model field integral behaves as in **fig. 1**. As the model generally has a different "slope" than the real field, the display of y versus I exhibits a residual non-zero slope, like on **fig. 2** (Note the change of scale in ordinate w.r.t. **fig. 1**).

Definition of increasing and decreasing branches:

On an increasing branch of the hysteresis loop the current I goes successively from zero to $+I_{max}$, or from zero to $-I_{max}$. On a decreasing branch the current goes successively from $+I_{max}$ to zero, or from $-I_{max}$ to zero. Throughout this paper we draw increasing branches as solid lines and decreasing branches as dashed lines, on every plot. Each curve is oriented, i.e. has a starting point and a time-ordered evolution, indicated in Table 2 and graphically shown by arrows.

Each branch has a linear part at low current, and a part at higher current where a loss of linearity, or saturation, appears. Increasing branches have better linearity (i.e extending to higher current) than decreasing branches. It is why we recommend the use of increasing branches for setting the quad currents in addition to a full cycling loop.

Definition of saturation or non-linearity:

We work on increasing branches only. At a given current I the saturation in absolute (i.e. in T.mm) is given by the difference Δy between the experimental value of $y(I)$ and the one extrapolated from the linear part of the branch; see **fig. 2**.
The saturation in relative (%) is obtained by dividing the previous difference by the measured field integral at this current.

(N.B. another convention could be to divide Δy by the maximum field integral $F_{meas}(I_{max})$).

Fig. 4 shows the actual curves obtained for the HRS quads with this choice of representation. The hysteresis area becomes visible. In order to best visualize non-linearity effects, the most suitable representation of the hysteresis loop is the one where the two extreme points $y(\pm I_{max})$ are brought approximately to zero in ordinate. This can be done by choosing a new differential variable:

$$y_1(I) \;=\; F_{meas}(I) \;-\; [\;\; F_{model}(I) \times (1. + \alpha) \;\;]$$

where α is a small coefficient for "tuning" the model. Doing such for the HRS quads with the following coefficients: α(Q1)=1.463e-2, α(Q2/Q3)=0.837e-2, one gets the plots in **fig. 5**. One clearly sees the similarity of behaviour of Q2 and Q3, and their marked difference with Q1.

4 Results

From **fig. 5** we extract the main results about field linearity and reproducibility presented below.

4.1 Field at I=0

The [remanent + persistent] field of the HRS quads, or in other words their hysteresis, is very small. When normalized to the field integral at maximum current, it yields the following values:

Q1: (0.35 T.mm / 1178 T.mm) = 3.0e-4
Q2: (1.65 T.mm / 1813 T.mm) = 9.1e-4
Q3: (1.31 T.mm / 1174 T.mm) = 11.1e-4 , or
(1.40 T.mm / 1570 T.mm) = 8.9e-4 (asymmetric cycle).

That is, hysteresis normalized to maximum field is three times bigger for Q2/Q3 than for Q1.

4.2 Field Linearity

The way to quantify the non-linearity, or saturation, on the hysteresis loop has been defined in section 3.

First, the linear part of the loop has to be fitted by a straight line (D).

For **Q1** it turns out that QMM alone does not allow to check the magnet linearity between 0 and 1000 A, due to the lack of data at intermediate currents. Assuming this linearity would be too simplistic. First, if one tries to draw a hand-made fit through all the points of an increasing branch on **fig. 5** (Q1), it seems hardly compatible with a straight line going from 0 to 1000 A.
Second, measurements have been performed on the HRS-Electron quads by John Lerose [2] with a Hall probe. These measurements indicate that Q1 is linear up to 600 A and shows a $\simeq$ 1.e-3 relative saturation at I=1000 A (the data extends to 1200 A only). We will use this information to constrain the linearity line of Q1. For example, in terms of y_1 variable, the straight line for the increasing branch (I>0) is constrained to go through the point located at :

abscissa: I= +999.62 A
ordinate: F = $y_1(I) + F_{meas}(I) \times$ 1.e-3 =
363.4038 - 1161.94*(999.62/3250)*(1+ 1.463e-2) + 363.4038*1.e-3
= 1.153 T.mm

For **Q2** our QMM data clearly shows a very good linearity up to $\sim$ 1200 A. We choose to fit a straight line through the four data points at I= 0, 400, 800, 1200 A. We get the fitted parameters below :

(incr. branch I<0) $y_1 = (-1.78 \pm 0.14) + (-1.39 \pm 0.18)10^{-3} \times I$
(incr. branch I>0) $y_1 = (+1.78 \pm 0.14) + (-1.41 \pm 0.18)10^{-3} \times I$

(Notice the good symmetry of the two fits).

For **Q3** our QMM data again shows good linearity up to $\sim$ 1200 A. We could do the same fitting procedure as for Q2, but this is less interesting. As the measured points are now on an asymmetric loop, results will not compare between the two increasing branches (I>0, I<0) and they will not compare to Q2.

So from now on, numbers will be quoted for Q2/Q3 jointly, although they are based on our Q2 data only, being of better quality than Q3.

The linear fits of (D) are displayed as dotted lines on **fig. 5** for Q1 and Q2. At a given current I, the vertical segment separating the experimental y_1 value and the straight line determines the saturation in absolute. The relative saturation is obtained by dividing this number by $F_{meas}(I)$.

Actual saturation values for Q1 and Q2 in absolute are displayed on **figs. 6** and **7**: as numbers on vertical segments, top-right quadrant. From these numbers we get the relative saturation plot of **fig. 8-a**, which summarizes the field linearity of the

[2] J.Lerose, private communication (1997).

HRS quads (for increasing branches only).

4.3 Reproducibility of Magnet Setting

The user wants to know how well the value of the magnetic field (or the field integral) is reproduced each time the current in the magnet is set to the same value I. This is what we call the setting reproducibility. We can also speak of field reproducibility.

Present operation of the HRS magnets is done without cycling. It means that for a given current I, the field integral lies somewhere within the limits defined by the QMM hysteresis loop, because it is the cycle corresponding to maximal current. But we don't know where exactly, because it depends of the previous history of the magnet, as illustrated schematically on **fig. 9**.

QMM data allows to set a maximal error on the setting reproducibility (or equivalently a maximal non-reproducibility of the setting), by measuring the distance between field integrals on the increasing and decreasing branches at current I. The error is maximized because our cycle is as large as possible.

Reproducibility data in absolute is reported on **fig. 6** and **7**: as numbers on vertical segments, bottom-left quadrant. The maximal relative error in setting reproducibility at current I is obtained by :

$$Err.max \;=\; |[\; y_1(I) \text{ (increas.branch)} \;- y_1(I) \text{ (decreas.branch)} \;]/\; F_{meas}(I) \;|$$

These results are summarized on **fig. 8-b**. Given the fact that during Hall A commissioning the current settings of the HRS do not go to their maximal value, it is likely that the actual seting reproducibility of the quads at present time is much better than what is presented here.

5 Conclusions

We have presented a detailed analysis of the hysteresis curves measured by QMM for the three HRS-Electron quads. From **fig. 8** some properties of Q1 and Q2/Q3 can be compared:

- Q1 has a better setting reproducibility than Q2/Q3 (due to different iron qualities?)
- Q2/Q3 have a better field linearity than Q1 (due to a higher field in Q1 yoke).

momentum setting of one HRS	approx.value of magnet current	non-linearity (relative to $F_{meas}(I)$	max. error of reproducibility (relative to $F_{meas}(I)$
$P_0 = 1$ GeV/c	Q1: 750 A Q2/Q3: 400 A	$< 1.e\text{-}3$ negligible	1.8e-3 7.e-3
$P_0 = 2$ GeV/c	Q1: 1500 A Q2/Q3: 800 A	2.e-3 negligible	1.e-3 2.5e-3
$P_0 = 3$ GeV/c	Q1: 2250 A Q2/Q3: 1200 A	3.e-3 negligible	0.5e-3 1.5e-3

Table 3: Main results for three HRS momentum settings.

As a summary, we report our determination of the field linearity and reproducibility of the quads for typical momentum settings in the HRS: see Table 3.

Appendix I

In Table 4 we report the numerical values of the 2N-field integrals measured by QMM on the hysteresis loop, together with the value of the magnet current for each run. The computation of this current is done according to a previous note [3]. Namely, we choose the most reliable reading of the current that was available in june 1996 during QMM measurements (i.e. from a ZFT), and the dump resistance correction has been made.

Uncertainties of the QMM measurements

What are the error bars associated with the numbers in Table 4?

1. The magnet current. For Q1, the uncertainty is $\Delta I/I_{max} \simeq 1 \times 10^{-5}$ with $I_{max} = 3250$ A, as given by the power supply specifications.
For Q2/Q3, we had more problems determining the magnet current when doing the mapping, as explained in the previous note [3]. We had several ways of measuring the current at each setting. By comparing them, and e.g. making a gaussian fit of their disagreement, we get: $\Delta I \simeq 0.4$ A (r.m.s), i.e. $\Delta I/I_{max} = 0.4/1850 = 2.2 \times 10^{-4}$ with $I_{max} = 1850$ A.
(N.B. this error ΔI is specific to the current reading at the time our mapping in 1996. It does not mean that it is the actual regulation level of Q2/Q3 power supplies. The latter one may be better).

2. The field integrals. The error bar on their measurement can be divided into two contributions:

- a class of systematic errors, that apply to each measured F in the same way (i.e. with the same sign). Among them we find: uncertainties in coils geometry, and errors related to the electronic chain (multiplexer + integrator): absolute calibration uncertainty, non-linearity, change of calibration versus gain setting. These errors may amount to $\Delta F(I)/F(I) =$ a few 10^{-4}, but they are not relevant for the present study, because they cancel for their most part in the difference or ratio of F's that we are dealing with.

- a class of random, statistical errors translating into a reproducibility limit of each QMM measurement. Among various contributions: intrinsic resolution of the V-to-F Converter, temperature variations, etc, the main one comes from the current fluctuation of the power supply during one run.

[3] "QMM Runs: Computation of the magnet current", Note of October 14th 1996.

A practical estimation of the error bar associated to F can be obtained from the measurements in Table 4, by checking the symmetry between $F(I)$ and $-F(-I)$ on the increasing (or decreasing) branches for each value of I. One must take care to normalize properly the two measurements to the same $|I|$.

For Q1 the maximum observed difference between $F(I)$ and $-F(-I)$ is 0.048 T.mm (lines 1 and 10 of Table 4). This value is much smaller than any of the numbers quoted in **fig. 6**. So our results on Q1 linearity and setting reproducibility are meaningful.

One also deduces a maximal error of reproducibility of the QMM/Q1 measurement itself: $\Delta F(I)/F(I_{max}) = 0.048/1178 = 4.1 \times 10^{-5}$.

For Q2/Q3 the maximum observed difference between $F(I)$ and $-F(-I)$ is 0.63 T.mm (1st line and last line of Table 4). It is not small compared to the absolute saturation data quoted in **fig. 7**. However it is an isolated point, every other observed difference being smaller than 0.1 T.mm. So, again we are confident in the results obtained for Q2/Q3 linearity and setting reproducibility.

The maximal error of reproducibility of the QMM/Q2 measurement itself is estimated as above: $\Delta F(I)/F(I_{max}) = 0.63/1813 = 3.4 \times 10^{-4}$.

Q1	Q2	Q3
F_{meas} in T.mm (I in Amps)	F_{meas} in T.mm (I in Amps)	F_{meas} in T.mm (I in Amps)
-1178.621 (-3249.08)	-1812.937 (1849.37)	-1174.267 (1197.48)
-1088.331 (-2999.10)	-1568.994 (1599.11)	-979.278 (997.98)
-726.240 (-1999.39)	-1177.181 (1198.98)	-783.998 (798.47)
-363.843 (-999.65)	-785.099 (799.14)	-588.435 (598.95)
-.346 (.00)	-392.831 (398.96)	-392.955 (399.41)
363.404 (999.62)	-1.652 (-.11)	-1.306 (-.31)
725.877 (1999.37)	390.081 (-399.09)	195.201 (-200.57)
1088.122 (2999.10)	783.054 (-799.17)	392.034 (-400.83)
1178.613 (3249.08)	1175.758 (-1199.13)	785.124 (-801.31)
1088.379 (2999.10)	1568.212 (-1599.09)	1178.209 (-1201.76)
726.242 (1999.42)	1813.154 (-1849.01)	1570.863 (-1602.15)
363.846 (999.65)	1569.153 (-1599.18)	1179.776 (-1201.76)
.348 (.00)	1177.221 (-1199.00)	787.192 (-801.31)
-363.399 (-999.65)	785.157 (-799.15)	394.713 (-400.83)
-725.881 (-1999.37)	392.836 (-398.98)	1.402 (.33)
-1088.123 (-2999.10)	1.658 (.11)	-390.586 (399.41)
-1178.613 (-3249.08)	-390.067 (399.07)	-782.606 (798.47)
	-783.075 (799.14)	-1174.464 (1197.48)
	-1175.762 (1199.12)	-1566.114 (1596.43)
	-1568.219 (1599.07)	
	-1813.204 (1849.00)	

Table 4: QMM data on hysteresis loops: 2N-field integral versus I for each quad.

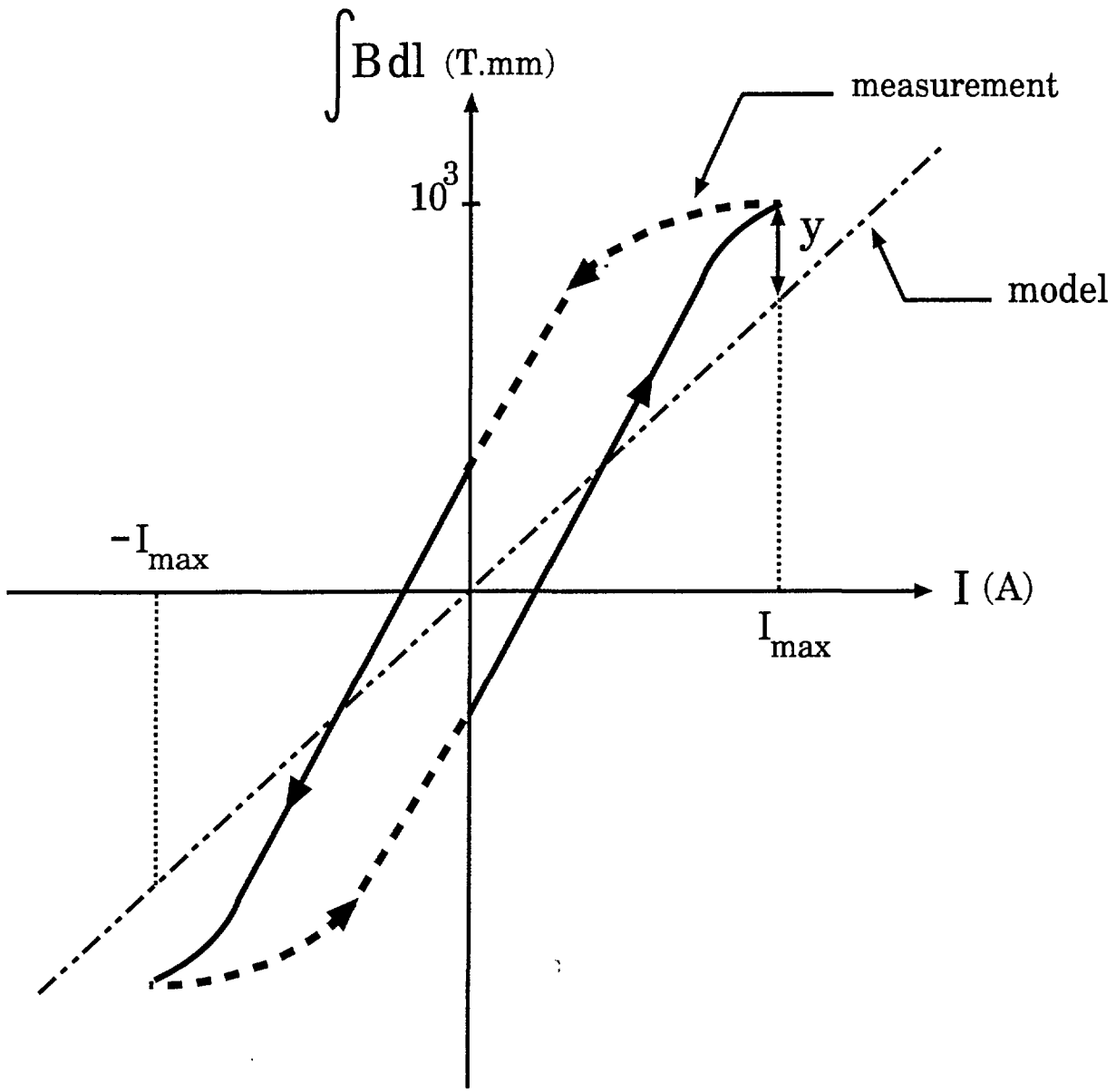

Figure 1: Hysteresis loop (schematic) in terms of field integrals F.

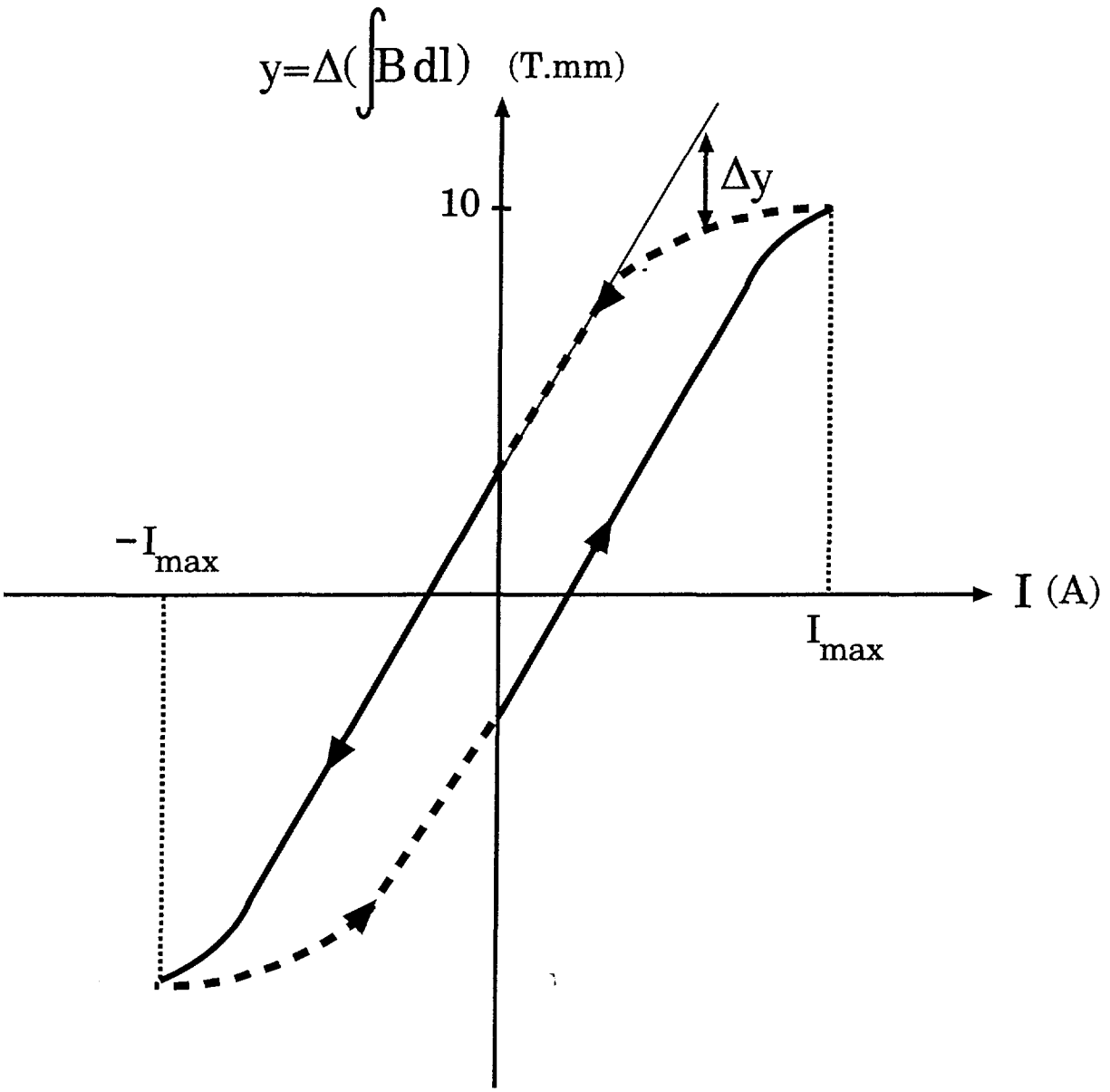

Figure 2: Hysteresis loop (schematic) in terms of differential variable $y = F_{meas} - F_{model}$.

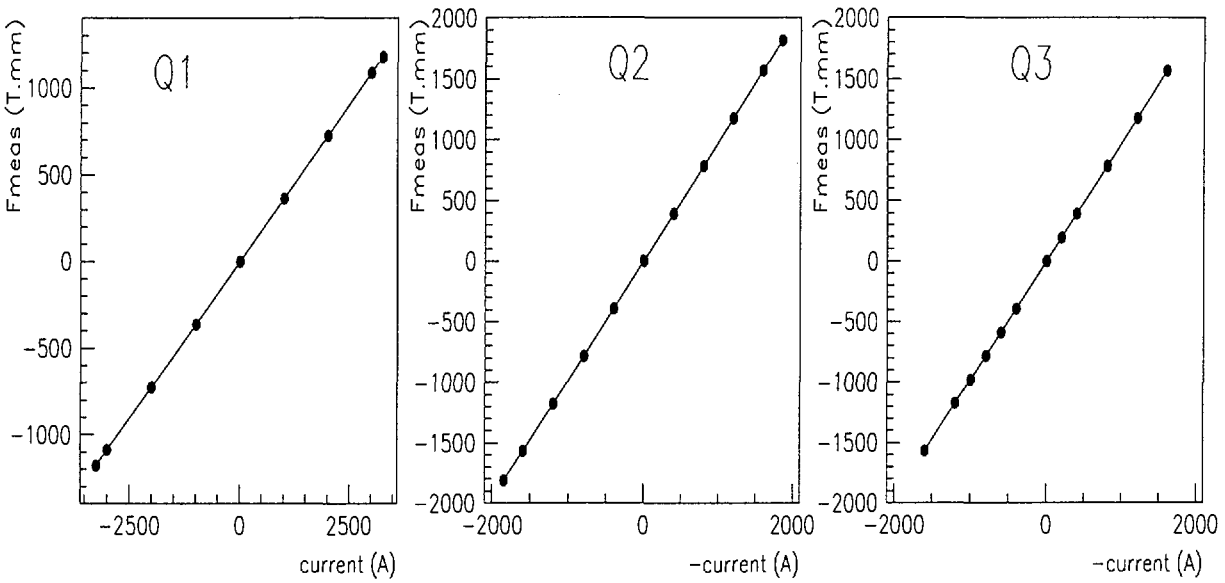

Figure 3: Hysteresis loop in terms of field integrals F for the HRS quads.

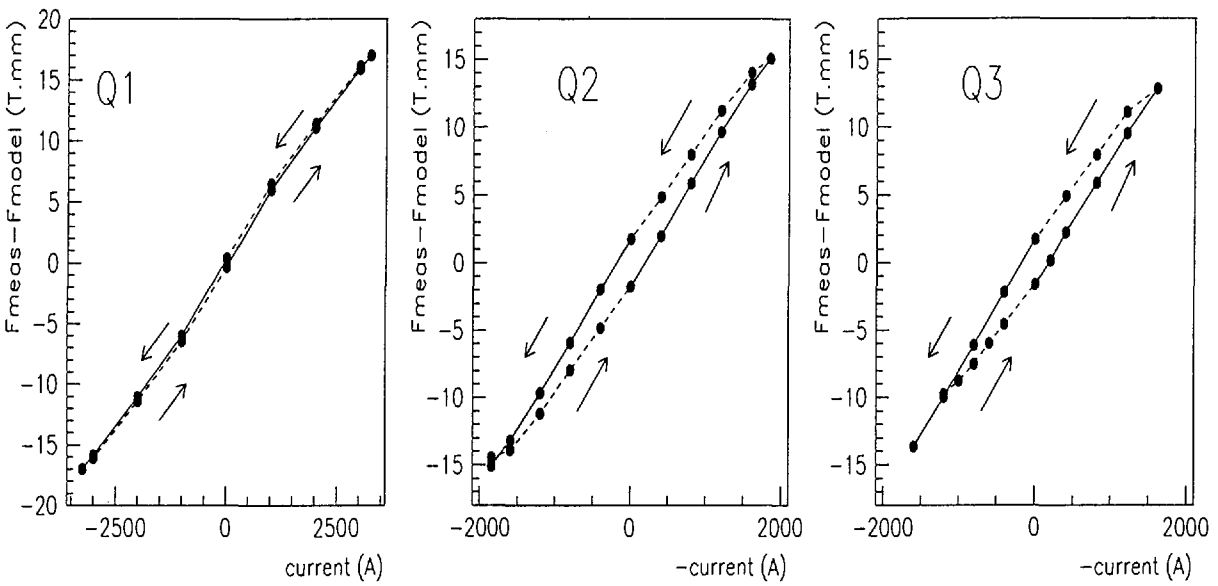

Figure 4: Hysteresis loop in terms of differential variable $y = F_{meas} - F_{model}$ for the HRS quads. The loop has been measured starting at $I = -3250/+1850/+1200$ A for Q1/Q2/Q3 and following the arrows.

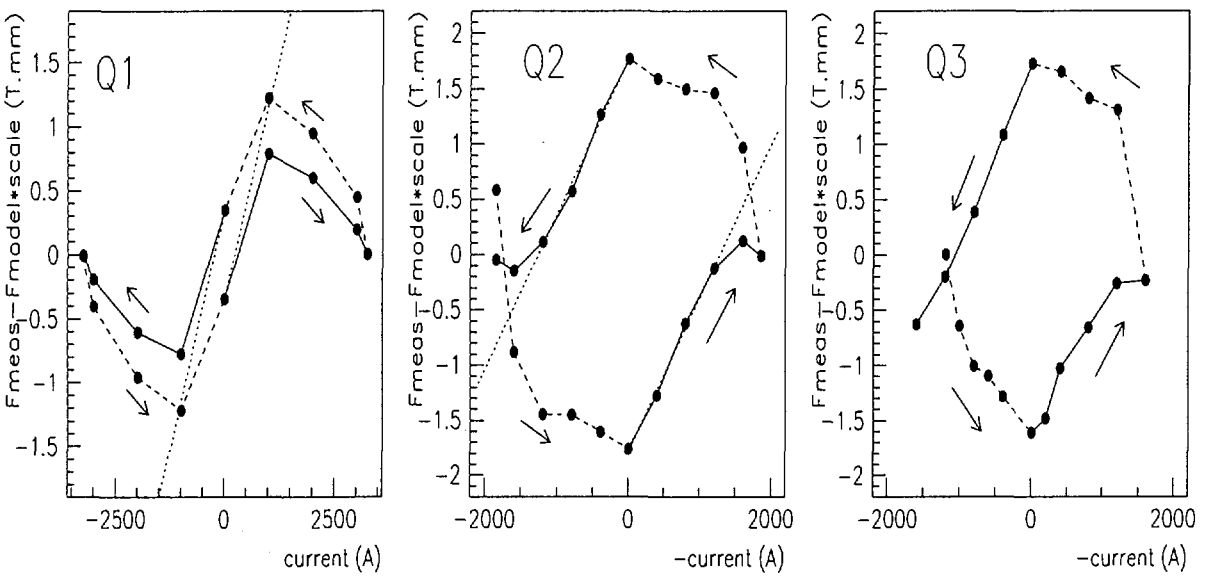

Figure 5: Hysteresis loop in terms of differential variable $y_1 = F_{meas} - F_{model} \times (1+\alpha)$ for the HRS quads. The variable y_1 is chosen such that $y_1(\pm I_{max}) \simeq 0$.
The loop has been measured starting at $I = -3250/+1850/+1200$ A for Q1/Q2/Q3 and following the arrows.

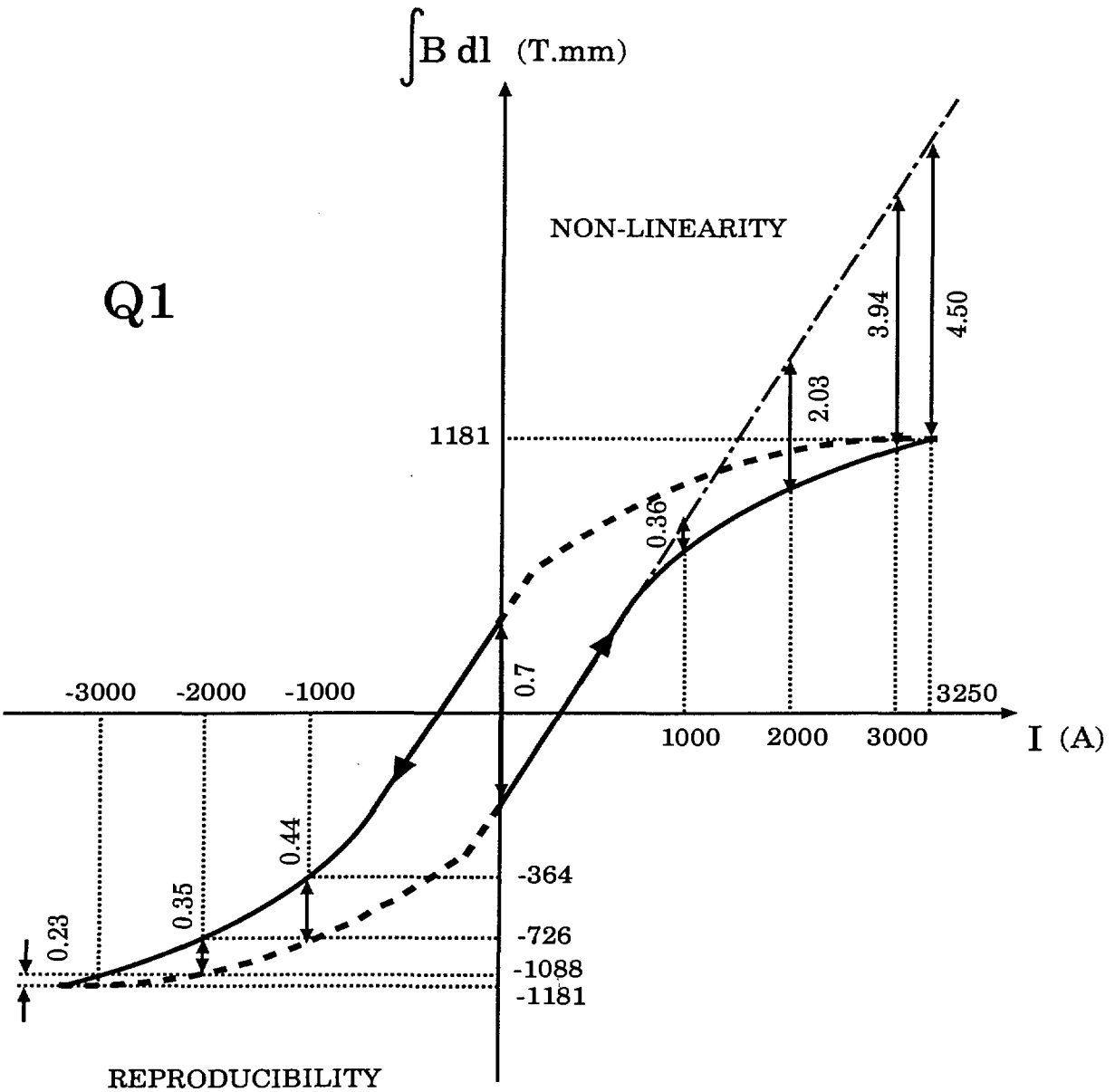

Figure 6: Hysteresis loop (schematic) with results on linearity and reproducibility for Q1. Numbers on the plot are in T.mm.

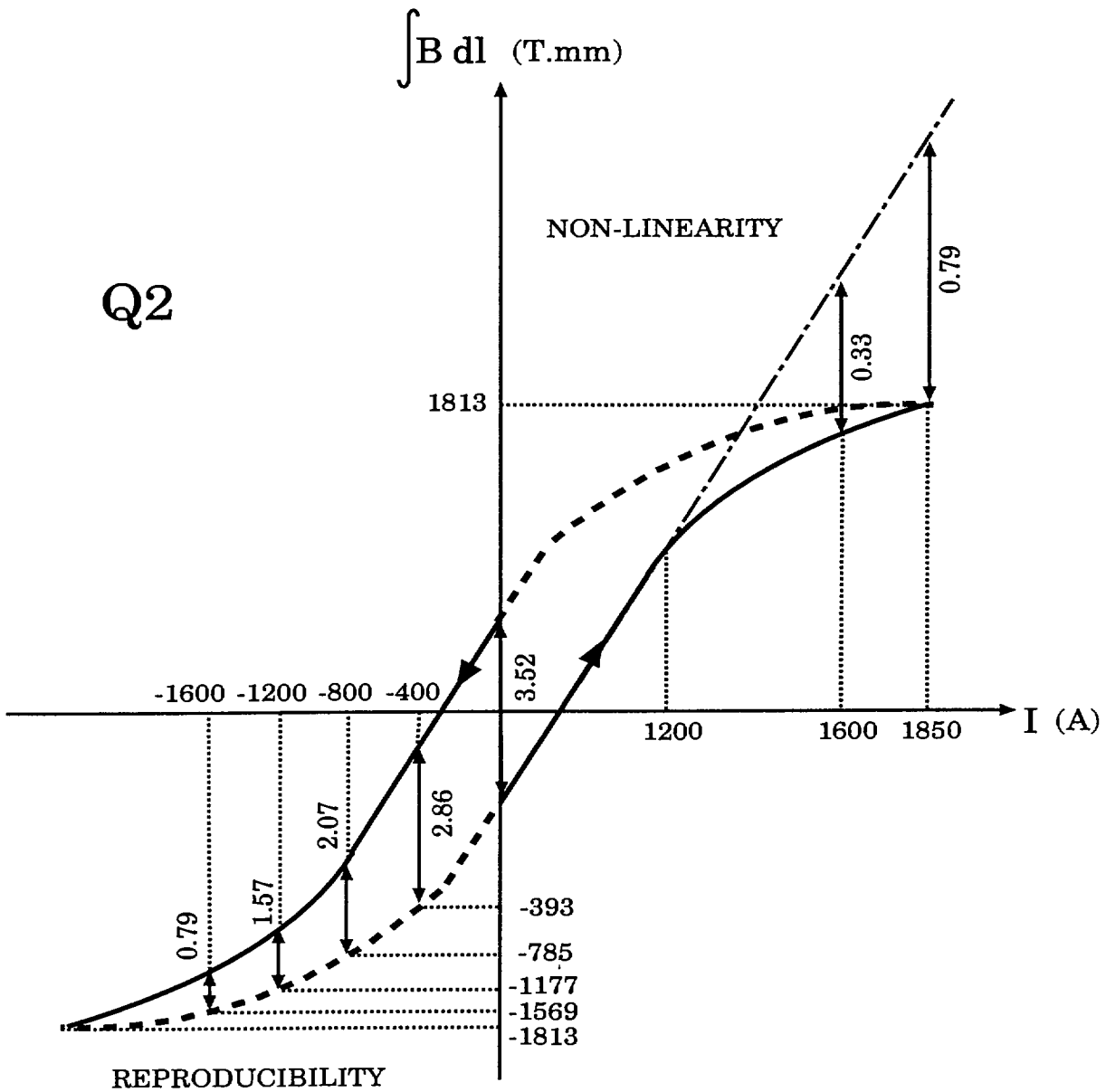

Figure 7: Same as fig. 6 but for Q2/Q3.

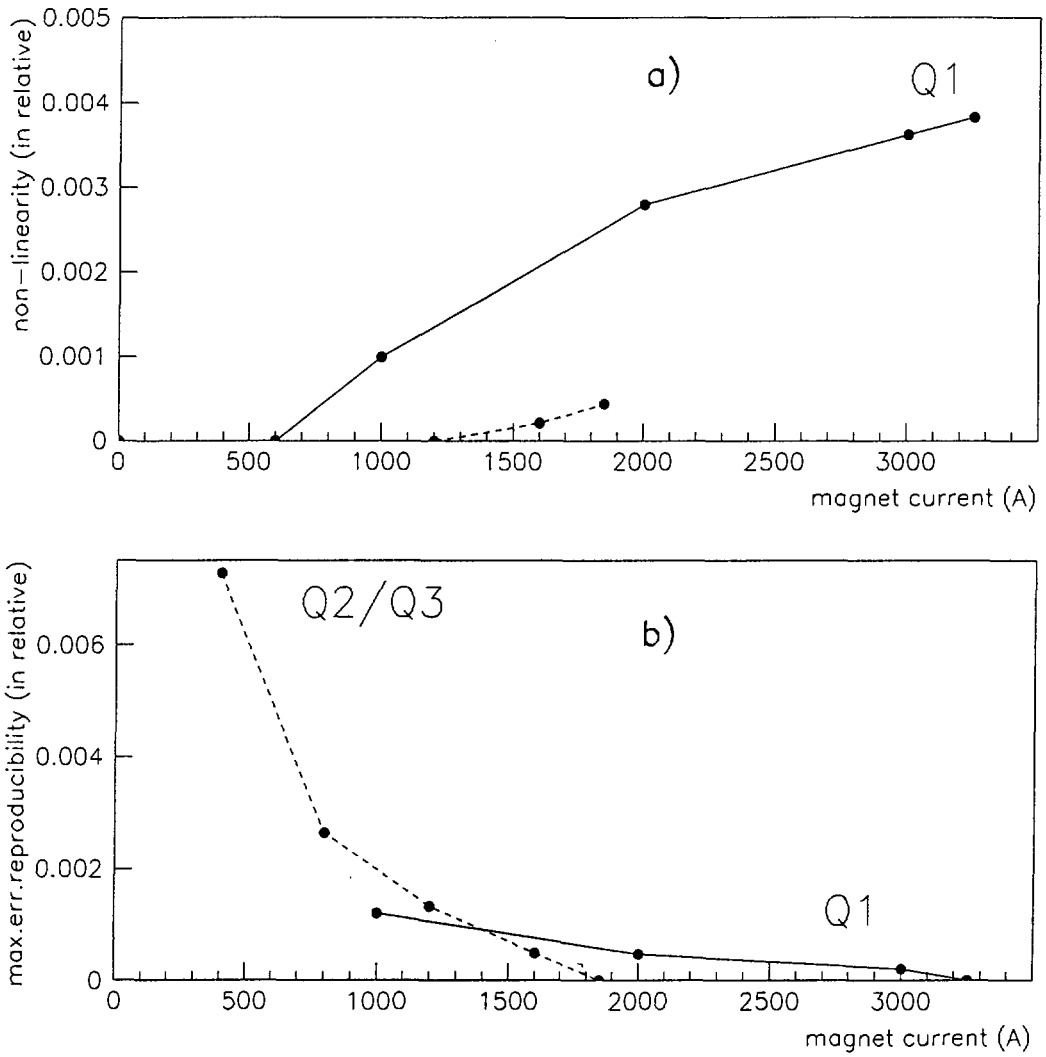

Figure 8: Summary of results on field linearity and setting reproducibility for Q1 and Q2/Q3.

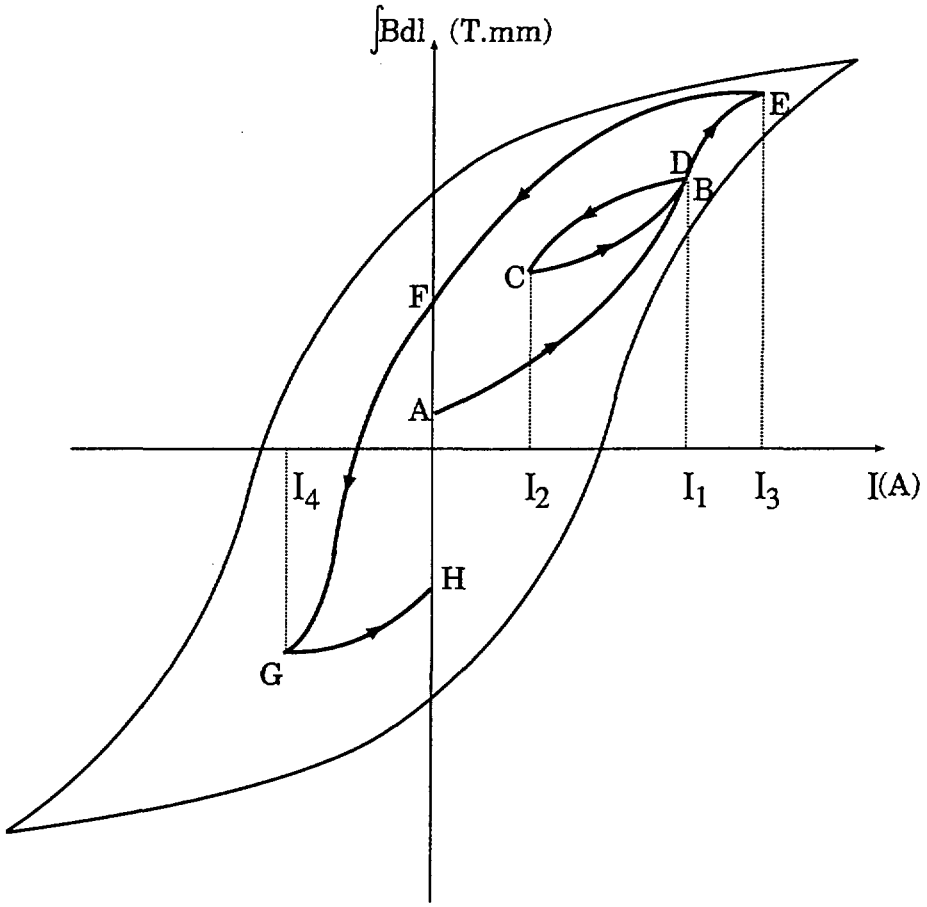

Figure 9: A schematic example of magnet history's influence on setting reproducibility.
Time-ordered steps: AB (lower arc)= ramping up from zero current to I_1. BC (upper arc): from I_1 to I_2. CDE: from I_2 to I_3. EFG: from I_3 to I_4. GH: back to zero current.